Volume 19, No 2 | International Journal of Radiation Research, April 2021

Dosimetric characterization of a new two-dimensional diode detector array used for stereotactic radiosurgery quality assurance

K. Yasui[1*], Y. Saito[2], S. Ogawa[3], N. Hayashi[4]

[1]*Fujita Health University, Faculty of Radiological Technology, School of Medical Sciences, 1-98 Dengakugakubo, Kutsukake-cho, Toyoake, Aichi 470-1192, Japan*
[2]*Department of Radiology, Fujita Health University Hospital, 1-98 Dengakugakubo, Kutsukake-cho, Toyoake, Aichi 470-1192, Japan*
[3]*Graduate School of Health Sciences, Fujita Health University, 1-98 Dengakugakubo, Kutsukake-cho, Toyoake, Aichi 470-1192, Japan*
[4]*Fujita Health University, Faculty of Radiological Technology, School of Medical Sciences, 1-98 Dengakugakubo, Kutsukake-cho, Toyoake, Aichi 470-1192, Japan*

► ***Original article***

Corresponding authors:
Keisuke Yasui, PhD.,
E-mail: *k-yasui@fujita-hu.ac.jp*

Revised: December 2019
Accepted: February 2020

Int. J. Radiat. Res., April 2021; 19(2): 281-289

DOI: 10.29252/ijrr.19.2.281

ABSTRACT

Background: The purpose of this study was to investigate the dosimetric characteristics of a new type of two-dimensional diode detector array used for quality assurance of stereotactic radiosurgery (SRS). ***Materials and Methods:*** The devices used in this study were the SRS MapCHECK detector and the StereoPHAN. The detector has 1013 diode detectors over an area of 77 x 77 mm^2. The reproducibility, dose linearity, dose rate dependencies, output factors (OPFs) and angular dependencies were investigated as dosimetric characteristics. The OPFs were measured and compared between AP and PA direction ranging from 0.5 x 0.5 to 7 x 7 cm^2. The angular dependencies were measured using 19 gantry angles. ***Results:*** The dose reproducibility and linearities showed sufficient performance of 6 MV and 10 MV. At 40 MU/min, there was a 1.3% difference from the ionization chamber measurements. For the flattening filter-free beam, there was no dose rate dependency from the 400 MU/minute to 2400 MU/minute, and the variation was within 0.5%. For small irradiation fields of 1 cm or less, the measured value of the SMC differed in AP and PA directions by up to 4.5%. The maximum gantry angle dependency of the detector was 5.3%. A maximum difference of -3.1% occurred between the measurements and TPS calculations. ***Conclusion:*** Results indicate that the new 2D diode detector is stable and useful for QA and end-to-end testing of SRS due to its excellent dose characteristics, high resolution and ease of handling when combined with the StereoPHAN.

Keywords: *SRS MapCHECK, dosimetric QA, end-to-end testing, 2D diode detector array, 2D measurement.*

INTRODUCTION

Two-dimensional (2D) detectors are now a standard, useful tool in advanced radiotherapy for Linac quality assurance (QA) and patient-specific QA. 2D detectors are efficient for many QA procedures because they can measure many point doses reliably, and are easy to set up [1,2]. While their advantages include dose stability, low error rates, time-saving in QA and economic advantages over the long term, a drawback when compared with film is their low resolution. To overcome these shortcomings, some small high-resolution 2D-detectors have

[Downloaded from ijrr.com on 2026-09-16]

[DOI: 10.52547/ijrr.19.2.5]

been developed based on liquid-filled or vented ionization chambers, or on diodes [3–7]. In practice, there are some limitations to each type of detector, and it is important to understand their respective characteristics. For a vented ionization chamber, the minimum size of the detector is limited to a size that allows sufficient signal strength to be obtained. Additionally, the measurement position of an ionization chamber is influenced by the detector volume which becomes large in regions having a steep dose gradient[8]. The liquid-filled ionization chamber offers dosimetry in a smaller volume than a vented ionization chamber, but such detectors have a directional (angular) dependency of up to 5% [4]. In addition, responses of the liquid-filled ionization chamber are influenced by the dose/pulse and mean photon energy [4]. Diodes are small detectors and thus suitable for verifying complex dose distributions. However, their responses are also influenced by the dose/pulse and mean photon energy, and a diode array may have significant angular dependences within ±10% [2,9,10].

kkmDose distributions in radiotherapy are often generated using various characteristic beam parameters such as the flattening-filter-free (FFF) beam. Stereotactic radiosurgery (SRS) is a high-precision radiotherapy technique, and the overall treatment needs to be within submillimeter accuracy [11]. Furthermore, the dose distribution of SRS is often complicated by using intensity-modulated radiotherapy (IMRT), volumetric-modulated arc therapy (VMAT), many small fields, and the presence of multiple targets. Thus, careful commissioning, patient-specific QA and end-to-end testing are essential to ensure the safety of these treatments. For this reason, many studies have been conducted on patient-specific QA with SRS in recent years, using high-resolution film for dosimetry [12–14]. Although these studies have shown good results and led to a variety of innovations, the film-based approach has disadvantages in terms of time and efficiency. Recently, Sun Nuclear Corporation (USA) released new equipment for SRS verification: the SRS MapCHECK detector (Sun Nuclear Corporation, USA: SMC) with the StereoPHAN phantom (Sun Nuclear Corporation, USA). The SMC is a high-density 2D diode array with 1013 silicon diodes, designed for patient-specific QA and end-to-end testing. The diode used in the SMC is a SunPoint2 diode (Sun Nuclear Corporation, USA) with a detection area of roughly 0.23 mm^2. As mentioned above, diode detectors are known to have dose rate and energy dependence. It is also important to clarify the basic characteristics of the new 2D diode array detector for the FFF beam, because many treatment plans using FFF beams are performed in SRS. In addition, the SMC is the first commercial 2D diode array detector to offer angular correction for each gantry angle. As far as we know, no scientific paper so far has examined the characteristics of this new diode array detector. This study aimed to clarify the various dosimetric characterizations of the SMC for conventional (with-flattening filter: WFF) and FFF beams. These results provide useful data for more effective use of the new diode array detector.

MATERIALS AND METHODS

Characterization of detector and phantom

The SMC is designed to be held by the StereoPHAN and is equipped with 1013 small diodes; the active detector area of each diode is 0.48×0.48 mm^2 and the active detector volume is 0.007 mm^3. The effective measurement area of the SMC is 77×77 mm^2 and the distance between the centers of the detectors is 2.47 mm at 45° (3.5 mm in-line diode spacing), so 55 detectors are contained in a 2×2 cm^2 treatment field. Figure 1 shows the physical specifications of the SMC and StereoPHAN. The SMC is able to perform absolute and relative dose analysis using SNC Patient Software (Sun Nuclear Corporation, USA). The supporting energies of the SMC are 6 MV and 10 MV with both WFF and FFF beams. The SMC is inserted into the StereoPHAN and can be rotated and measured at any angle for axial-sagittal viewing. The physical dimensions (length/width/height) of the SMC and the StereoPHAN are 320×105×45 mm^3 and 518×276×323 mm^3. The 162 mm cylinder of the

[Downloaded from ijrr.com on 2026-09-16]

[DOI: 10.52547/ijrr.19.2.5]

StereoPHAN can be rotated through 360°, which allows the measurement of an arbitrary section using the SMC (figure 1).

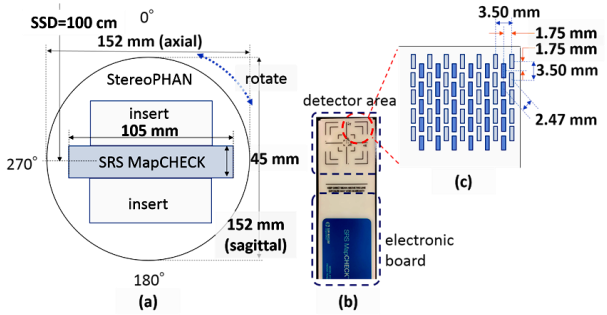

Figure 1. Schematic diagram and dimensions of the SMC and inserts within the StereoPHAN **(a)**, appearance of the SMC **(b)**, internal detector arrangement and geometry **(c)**.

According to the AAPM Task Group 218 report [2], the angular dependence of a general diode array detector is within 10%, and angular dependence should be taken into account for the 2D array measurement. The angular dependencies of diode arrays result from the sensitivity of diode detector to the incident beam angle and non-water equivalence of the diode array (circuit boards, other detectors and air gaps). The SMC is the first commercial detector that can automatically correct angular dependencies. Any angular correction algorithm needs to know the incidence beam angle; however, the SMC allows estimation of the incident beam angle using only the data measured by the device with two printed circuit boards. As a preparatory step for measuring using the SMC, array calibration is performed from both anterior-posterior (AP) and posterior-anterior (PA) directions, and these data are used for angular dependency calibration. The angular dependency correction for the diode response is performed by constructing and applying an array calibration, which is a weighted sum of AP and PA array calibrations. The angular dependencies of the SMC caused by differences in water equivalence are handled by converting computer tomography (CT) values on a treatment planning system. The weighting factor of the sum of the sensitivity of diode and non-water equivalence is a function of the incident beam angle. In clinical use, angular dependency corrections are calculated and applied for each beam-on update.

Experimental setup for measurements and analysis of dosimetric characterization

All measurements were carried out using 6 MV WFF, 10 MV WFF, 6 MV FFF and 10 MV FFF with a TrueBeam (Varian Medical Systems, USA). The reference conditions for 6 MV WFF, 10 MV WFF, 6 MV FFF, and 10 MV FFF were 5 × 5 cm^2, source-surface-distance (SSD) 100 cm and 100 monitor-unit (MU). Reference dose rates were 500 MU/min for the WFF beam, 1000 MU/min for the 6 MV FFF, and 1600 MU/min for the 10 MV FFF. These reference conditions were used for the array calibration.

The reproducibility of the output of the SMC was investigated by taking five measurements under the reference conditions. Regarding reproducibility, a dose of more than 0.5 Gy was used, all 1013 detectors were considered separately, and the relative standard deviation (RSD) and its dispersion for each detector were analyzed. The dose linearity of each beam from 5 MU to 1000 MU was assessed using the same measurement setup. The measured MU values were 5, 10, 20, 30, 50, 100, 200, 300, 500, 7000, and 1000 MU.

The dose rate dependences were measured for 5 × 5 cm^2 and 100 MU at nominal dose rates of 40, 100, 300 and 500 MU/min for the WFF beam, 400, 600, 800, 1000, 1200 and 1400 MU/min for 6 MV FFF, and 400, 800, 1200, 1600, 2000 and 2400 MU/min for 10 MV FFF.

The OPFs were assessed by delivering 100 MU from 0.5×0.5 cm^2 to 7×7 cm^2 square fields with AP and PA planes to verify the variation due to the difference of the incident surface. The dose rate dependency and the OPF were compared with ionization chamber measurements. The dose rate dependencies were measured using a 0.125 cc Semiflex chamber (PTW 31010, Germany).

The angular dependencies were measured using 19 gantry angles. The angles of incidence near the horizontal direction of the detector (near 90°) were obtained at a fine pitch gantry angle, and the usefulness of the gantry angle correction was verified. We used a treatment planning system RayStation (TPS; version 8,

[Downloaded from ijrr.com on 2026-09-16]

[DOI: 10.52547/ijrr.19.2.5]

RaySearch) to verify the angular dependencies of the SMC. CT images of the SMC within the StereoPHAN were taken to calculate TPS doses. The Hounsfield unit (HU) of CT images of the StereoPHAN with the SMC was overridden to a density of 1.2 g/cm^3, which is the recommended value to compare dose distributions. In order to compare the SMC measurements with the TPS calculations, the absolute dose value of the SMC was calibrated with the planned dose using the 0° beam.

RESULTS

The differences between the array calibration factors in the AP and PA directions were 7.15 ± 0.43% for 6 MV and 5.46 ± 0.38% for 10 MV. The array calibration factors for each detector were generally close, and no difference in sensitivity was observed among the detectors. Table 1 shows the average and maximum RSDs of detectors irradiated over 0.5 Gy and all detectors. For the detectors in the irradiation field, the average value of RSD was 0.13% and the maximum value was 0.2%. The RSDs for all detectors were less than 1.06%. The detector with the largest RSD at each energy was a detector irradiated very a low dose, less than 3 cGy. There was no energy dependency in the variation of the reproducibility.

Figure 2 shows the dose linearities of WFF and FFF beams from 5 to 1000 MU of center detector. The right figure shows an enlarged low dose area of less than 100 MU. The low MU regions of 5, 10, 20, and 30 represent the average of three measurements. The coefficients of determination (R^2) were 1.000 for all beams, and the results showed good dose linearity.

The results of the dose rate dependencies are shown in Figure 3. For the FFF beam, there were negligible dose rate dependencies from the minimum to the maximum dose rates, and the variations were within 0.5%. In contrast, for the WFF beam, the response decreased at low dose rates, and the maximum difference from the ionization chamber was 1.3% at 40 MU/min.

Table 1. Average and maximum RSDs and dispersion of the RSDs of detectors irradiated over 0.5 Gy and all detectors.

	More than 0.5 Gy			All detectors		
(%)	Average RSD	Dispersion of the RSD	Maximum RSD	Average RSD	Dispersion of the RSD	Maximum RSD
6 MV WFF	0.06	0.02	0.11	0.18	0.13	0.86
10 MV WFF	0.06	0.03	0.14	0.23	0.19	1.02
6 MV FFF	0.13	0.03	0.20	0.23	0.15	1.06
10 MV FFF	0.08	0.02	0.15	0.20	0.14	0.82

The OPFs for 6 and 10 MV / WFF and FFF beams are shown in table 2. Table 2 shows the OPFs measured using SMC of AP and PA directions and differences between AP or PA directions of the SMC. For fields larger than 2×2 cm^2, the OPFs between AP and PA direction agreed well, within 1%. For small irradiation fields of 1 cm or less, the measured value of the SMC differed in AP and PA directions by up to 4.5%.

Figure 4 shows the angular dependencies measured using the SMC. We set the reference beam angle to 0°, i.e., perpendicular to the SMC, and calculated the angular dependencies of dose differences to 0°. For angles except near-horizontal, the maximum difference was 1.2% and the angular dependencies were small. Data acquired in the horizontal direction relative to the detector array, i.e., at 80° - 95° and 270°, showed a random variation relative to the gantry angle, with a maximum difference of -5.3% for the 10 MV WFF beam. Compared with the TPS, there was a maximum difference of -3.87% between the SMC measurements and the TPS calculations, and the worst gamma value (1 mm/2%) was 49.3% for the 10 MV WFF beam

[Downloaded from ijrr.com on 2026-09-16]

[DOI: 10.52547/ijrr.19.2.5]

at 90° (table 3). Figure 5 shows a comparison of dose distributions between the SMC and the TPS of the 0° beam of each energy and the 85° and 90° beams of the 10 MV WFF. The dose distributions from the 0° beam agreed very well for all energies of WFF and FFF. This also confirmed that the resolution of the SMC was high and that the dose distributions in the penumbra area were obtained with high accuracy (figure 5a-d). Except for the horizontal line beams, all dose distributions were perfectly consistent with the relative dose (gamma pass: 1 mm/2%, pass rate: 100%). These results suggested that the decrease in the pass rate of these beams reflects the deviation of the central dose. In contrast, as expected, the slopes of the dose distribution did not agree between the SMC measurements and TPS calculations for the 90° and 270° beams (figure 5e and 5f).

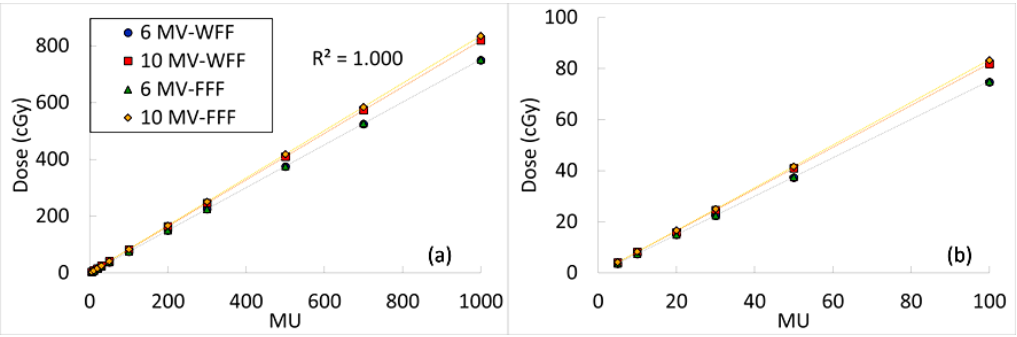

Figure 2. Dose linearities of WFF and FFF beams from 5 to 1000 MU **(a)**. An enlarged low dose area of less than 100 MU **(b)**.

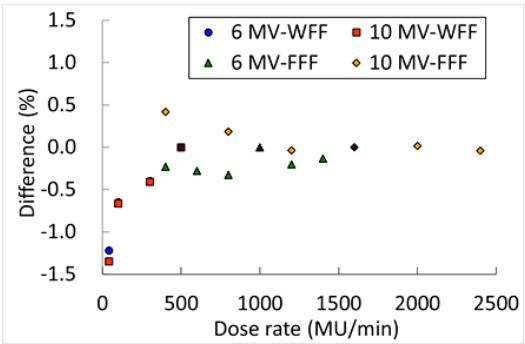

Figure 3. Dose rate dependencies of WFF and FFF beams from 40 to 2400 MU/min. Reference dose rates were 500 MU/min for the WFF beam, 1000 MU/min for the 6 MV FFF, and 1600 MU/min for the 10 MV FFF.

Table 2. Differences between OPF of AP or PA directions of the SMC and the ionization chamber measurements.

Square field size (cm^2)	6 MV WFF			6 MV FFF		
	AP	PA	Difference (%)	AP	PA	Difference(%)
0.5	0.315	0.310	0.55	0.254	0.235	1.90
1.0	0.695	0.741	-4.54	0.635	0.649	-1.42
2.0	0.883	0.891	-0.85	0.882	0.897	-1.49
3.0	0.931	0.927	0.34	0.948	0.938	1.06
5.0	1.000	1.000	-	1.000	1.000	-
7.0	1.061	1.056	0.55	1.044	1.044	0.06
Square field size (cm^2)	**10MV WFF**			**10MV FFF**		
	AP	PA	Difference (%)	AP	PA	Difference (%)
0.5	0.323	0.308	1.56	0.279	0.256	2.37
1.0	0.704	0.745	-4.10	0.663	0.680	-1.67
2.0	0.881	0.882	-0.09	0.895	0.903	-0.87
3.0	0.933	0.920	1.24	0.951	0.949	0.24
5.0	1.000	1.000	-	1.000	1.000	-
7.0	1.061	1.053	0.74	1.036	1.031	0.46

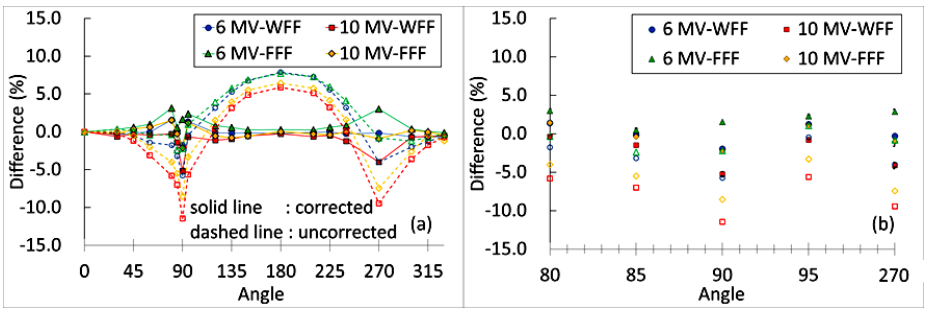

Figure 4. Angular dependencies measured using the SMC for 19 gantry angles **(a)** and enlarged view of angles near-horizontal to the detector **(b)**. The difference is relative to the reference beam of the 0° beam. Solid lines and closed symbols showed corrected data and dashed lines and open symbols showed uncorrected data.

[Downloaded from ijrr.com on 2026-09-16]

[DOI: 10.52547/ijrr.19.2.5]

Table 3. Differences between the SMC measurements and TPS calculations with gantry angle. Gamma shows gamma-index pass rate (1 mm /2%). Dose differences are calculated by the following formula: (SMC – TPS) / TPS x 100 [%].

Gantry angle (°)	Local percentage difference from chamber measurements (%)			
	6 MV WFF		6 MV FFF	
	Gamma (1 mm/2%)	Dose difference (%)	Gamma (1 mm/2%)	Dose difference (%)
0	100.0	0.00	100.0	0.00
45	100.0	0.81	100.0	0.66
80	80.6	1.65	63.1	2.77
85	95.3	0.49	95.5	0.90
90	54.6	-0.93	55.4	1.76
95	92.6	1.57	91.8	2.28
135	100.0	0.46	100.0	1.10
180	100.0	-0.35	100.0	0.71
270	59.7	-0.35	58.9	1.94
Gantry angle (°)	10 MV WFF		10 MV FFF	
	Gamma (1 mm/2%)	Dose difference (%)	Gamma (1 mm/2%)	Dose difference (%)
0	100.0	0.00	100.0	0.00
45	100.0	0.67	100.0	0.81
80	95.7	0.08	76.9	1.63
85	96.7	-0.81	94.6	0.16
90	49.3	-3.87	52.8	-1.24
95	93.0	-0.24	92.0	1.36
135	100.0	-0.31	100.0	0.69
180	100.0	0.87	100.0	0.92
270	52.1	-3.46	56.0	-0.95

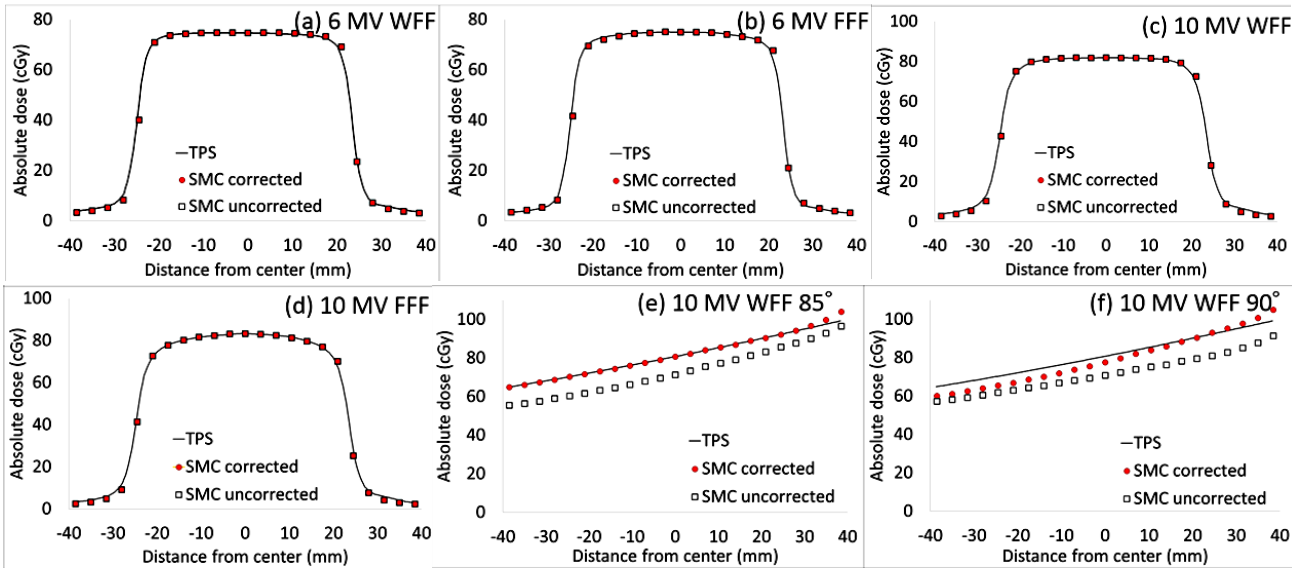

Figure 5. Comparison of dose distributions between the SMC and TPS using 0° beam of each energy **(a-d)** and 85° and 90° beams of 10 MV WFF **(e, f)**. Closed symbols showed corrected data and open symbols showed uncorrected data.

DISCUSSION

We examined various dosimetric characterizations of the SMC for WFF and FFF beams of 6 MV and 10 MV. Our results indicate that the SMC is a stable detector and useful for QA and end-to-end testing of SRS. As shown in table 1 and figure 2, the responses of the detector for 6 MV

[Downloaded from ijrr.com on 2026-09-16]

[DOI: 10.52547/ijrr.19.2.5]

and 10 MV were stable and did not depend on the beam type. Furthermore, the dose linearity and reproducibility showed sufficient performance. The results of array calibration performed in the AP and PA directions indicated that the diode detector demonstrates incident angle dependency on the beam energy, and the sensitivity variation among the detectors was small. As for the reproducibility and dose linearity, the results were equivalent to those of previous studies that evaluated the performance characteristics of two-dimensional detectors, and confirmed that the performance is sufficient [15, 16].

As in previous reports [7, 17, 18], an under-response of the diode detector was observed at low dose rates, which is a known limitation of diode detectors. The WFF beam was examined up to at least 40 MU/min, which is 29-33 cGy/min. Our results showed almost the same dose rate dependency as reported by Letourneau *et al.* [16], and the basic performance of the diode detector was considered to be similar for dose rate. This under-response is due to the fact that the recombination center near the band edge of silicon becomes empty and some of the generated charge carriers are lost to these traps [19]. The available dose rate for the TrueBeam FFF beam used in this study was 400 - 2400 MU/min, and within this range, the dose rate dependencies were within 0.5%. Since the dose rate decreases during irradiation with the VMAT, it is important to understand the under-response due to this decrease in dose rate.

The difference of the OPFs between AP and PA direction of small fields of 1×1 cm^2 or less was up to 4.54%. This larger difference for smaller fields was considered to be caused by a sensitivity change of the diode direction. Many studies have examined dosimetry in small static fields, reporting that the response characteristic of the detector changes due to a volume effect, a change in the energy spectrum in a small radiation field, or a change influence by using a solid phantom [20–25]. From the TRS report 483 [26], the maximum uncertainty in measurements of a small irradiation field of 0.5×0.5 cm using a Sun Nuclear EDGE diode was estimated at about ±3.5%. However, the internal structure of the SMC is complicated and the detectors are close to each other, and the fluence change due to the material of the SMC and the StereoPHAN has not been clarified. It will be necessary to clarify these points by Monte Carlo simulation or measurements using other detectors.

As shown in figures 4, 5 and table 3, the gantry angle dependencies of the SMC were within 5.3% relative to 0°, and a maximum difference of -3.1% occurred between the SMC measurements and TPS calculations. Previous studies using the diode detector array, MapCHECK, and MapCHECK2, reported gantry angle dependencies of 25-40% for horizontal incidence beams [27–29]. In these reports, the incidence angle dependency was 5 - 10% even with irradiation from an oblique field, From the data without the angle correction (indicated as dotted lines in figure 4), it can be seen that the angle dependency of about 15% occurs in the horizontal beam when the correction is not performed, which is greatly improved by the angle correction of the SMC. Improvements include better detector performance, the shape of the StereoPHAN, and the effect of automatic gantry angle correction. Gantry angle dependencies of 5-15% were also reported for other two-dimensional detectors using ionization chambers [4,15,18], and excellent results were obtained in the present study. In comparison with the treatment planning system, results of 80° showed a 1.6 ~ 2.7% difference in the central dose, which resulted in a lower gamma-index pass rate. In addition, the SMC can be used in combination with the StereoPHAN to rotate the detection surface and obtain data at any angle. A phantom must be uniformly overwritten on TPS; however, patient verification can also be performed while avoiding the high-impact horizontal incidence beam angle.

CONCLUSION

We reported various dosimetric characterizations of the SMC for WFF and FFF beams. The SMC showed excellent dose

[Downloaded from ijrr.com on 2026-09-16]

[DOI: 10.52547/ijrr.19.2.5]

characteristics even in comparison with other two-dimensional array type detectors. Although its utility for actual clinical patient-specific QA needs to be verified in the future because of the dose dependencies by irradiation field and incident direction, good results may be expected because of the superior characteristics compared with existing 2D detector arrays.

ACKNOWLEDGMENTS

The authors are grateful to TOYO MEDIC for lending us a detector for this research.

Compliance with ethical standards

This research did not receive any specific grant from funding agencies in the public, commercial, or not-for-profit sectors.

Conflicts of interest**:** *Declared none.*

REFERENCES

1. Low DA, Moran JM, Dempsey JF, Dong L, Oldham M (2011) Dosimetry tools and techniques for IMRT. *Med Phys,* ***38****: 1313–1338.*
2. Moyed M, Arthur O, Dimitris M, *et al.* (2018) Tolerance limits and methodologies for IMRT measurement ‐ based verification QA: Recommendations of AAPM Task Group No. 218. *Med Phys,* ***45****: e53–e83.*
3. Poppe, B, Stelljes TS, Looe HK, Chofor N, Harder D, Willborn K (2013) Performance parameters of a liquid filled ionization chamber array: Properties of a liquid filled ionization chamber array. *Med Phys,* ***40****: 082106.*
4. Markovic M, Stathakis S, Mavroidis P, Jurkovic IA, Papanikolaou N (2014) Characterization of a two-dimensional liquid-filled ion chamber detector array used for verification of the treatments in radiotherapy. *Med Phys,* ***41****(5).*
5. Van Esch A, Huyskens DP, Basta K, Evrard M, Ghislain M, Sergent F (2014) The Octavius1500 2D ion chamber array and its associated phantoms: Dosimetric characterization of a new prototype. *Med Phys,* ***41****(9).*
6. Anvari A, Aghamiri SMR, Mahdavi SR, Alaei P (2014) Statistical analysis on 2D array of ion chamber performance. *J Radiother Pract,* ***14****: 194–201.*
7. Biasi G, Petasecca M, Guatelli S, Hardcastle N, Carolan M, Perevertaylo V, Kron T, Rosenfeld AB (2018) A novel high-resolution 2D silicon array detector for small field dosimetry with FFF photon beams. *Phys Med,* ***45****: 117–126.*
8. Stelljes TS, Harmeyer A, Reuter J, Looe HK, Chofor N, Harder D, Poppe B (2015) Dosimetric characteristics of the novel 2D ionization chamber array OCTAVIUS Detector 1500. *Med Phys,* ***42****: 1528–1537.*
9. Masi L, Casamassima F, Doro R, Francescon P (2011) Quality assurance of volumetric modulated arc therapy: Evaluation and comparison of different dosimetric systems. *Med Phys* ***38****: 612–621.*
10. Esch A Van, Clermont C, Devillers M, Iori M, Huyskens DP (2007) On-line quality assurance of rotational radiotherapy treatment delivery by means of a 2D ion chamber array and the Octavius phantom. *Med Phys,* ***34****: 3825–3837.*
11. Halvorsen PH, Cirino E, Das IJ, Garrett JA, Yang J, Yin F, Fairobent LA (2017) AAPM-RSS Medical Physics Practice Guideline 9.a. for SRS-SBRT. *J Appl Clin Med Phys,* ***18****:10–21.*
12. Ahmed S, Kapatoes J, Zhang G, Moros EG, Feygelman V (2018) A hybrid volumetric dose verification method for single-isocenter multiple-target cranial SRS. *J Appl Clin Med Phys,* ***19****: 651–658*
13. Brezovich IA, Wu X, Popple RA, Covington E, Cardan R, Shen S, Fiveash J, Bredel M, Guthrie B (2019) Stereotactic radiosurgery with MLC-defined arcs: Verification of dosimetry, spatial accuracy, and end-to-end tests. *J Appl Clin Med Phys,* ***20****: 84–98.*
14. Covington EL, Snyder JD, Wu X, Cardan RA, Popple RA (2019) Assessing the feasibility of single target radiosurgery quality assurance with portal dosimetry. *J Appl Clin Med Phys,* ***20****: 135–140*
15. Syamkumar SA, Padmanabhan S, Sukumar P, Nagarajan V (2012) Characterization of responses of 2d array seven29 detector and its combined use with octavius phantom for the patient-specific quality assurance in rapidarc treatment delivery. *Med Dosim,* ***37****: 53–60.*
16. Spezi E, Angelini AL, Romani F, Ferri A (2005) Characterization of a 2D ion chamber array for the verification of radiotherapy treatments. P*hys Med Biol,* ***50****: 3361–3373.*
17. Létourneau D, Gulam M, Yan D, Oldham M, Wong JW (2004) Evaluation of a 2D diode array for IMRT quality assurance. *Radiother Oncol,* ***70****: 199–206.*
18. Sekar Y, Thoelking J, Eckl M, Kalichava I, Sihono DSK, Lohr F, Wenz F, Wertz H (2018) Characterization and clinical evaluation of a novel 2D detector array for conventional and flattening filter free (FFF) IMRT pre-treatment verification. Z *Med Phys,* ***28****:134–141.*
19. Saini AS and Zhu TC (2004) Dose rate and SDD dependence of commercially available diode detectors. *Med Phys,* ***31****: 914–924.*
20. Alfonso R, Andreo P, Capote R, *et al.* (2008) A new formalism for reference dosimetry of small and nonstandard fields. *Med Phys,* ***35****: 5179–5186.*
21. Czarnecki D and Zink K (2013) Monte Carlo calculated correction factors for diodes and ion chambers in small photon fields. *Phys Med Biol,* ***58****: 2431–2444.*
22. Ralston A, Liu P, Warrener K, McKenzie D, Suchowerska N (2012) Small field diode correction factors derived using an air core fibre optic scintillation dosimeter and EBT2 film. *Phys Med Biol,* ***57****: 2587–2602.*
23. Lechner W, Palmans H, Sölkner L, Grochowska P, Georg D

[Downloaded from ijrr.com on 2026-09-16]

[DOI: 10.52547/ijrr.19.2.5]

(2013) Detector comparison for small field output factor measurements in flattening filter free photon beams. *Radiother Oncol,* ***109****: 356–360.*

24. Dieterich S and Sherouse GW (2011) Experimental comparison of seven commercial dosimetry diodes for measurement of stereotactic radiosurgery cone factors. *Med Phys,* ***38****: 4166–4173.*
25. Seuntjens J, Olivares M, Evans M, Podgorsak E (2005) Absorbed dose to water reference dosimetry using solid phantoms in the context of absorbed-dose protocols. *Med Phys,* ***32****: 2945–2953.*
26. Palmans H, Andreo P, Christaki K, Huq M SJ (2017) Dosimetry of small static fields used in external beam radiotherapy: An IAEA-AAPM International code of practice for reference and relative dose determination. Int. At. Energy Agency
27. Jursinic PA, Sharma R, Reuter J (2010) MapCHECK used for rotational IMRT measurements: Step-and-shoot, Tomotherapy, RapidArc. *Med Phys,* ***37****: 2837–2846.*
28. Keeling VP, Ahmad S, Jin H (2013) A comprehensive comparison study of three different planar IMRT QA techniques using mapCHECK 2. *J Appl Clin Med Phys,* ***14****:222–233.*
29. Jin H, Keeling VP, Johnson DA, Ahmad S (2014) Interplay effect of angular dependence and calibration field size of MapCHECK 2 on RapidArc quality assurance. *J Appl Clin Med Phys,* ***15****: 80–92.*

[Downloaded from ijrr.com on 2026-09-16]

[DOI: 10.52547/ijrr.19.2.5]

[DOI: 10.52547/ijrr.19.2.5] [Downloaded from ijrr.com on 2026-09-16]